


RESEARCH ARTICLE

Resting-state and task-based centrality of dorsolateral prefrontal cortex predict resilience to 1 Hz repetitive transcranial magnetic stimulation

Sophie M. D. D. Fitzsimmons^{1,2}  | Linda Douw² | Odile A. van den Heuvel^{1,2} | Ysbrand D. van der Werf² | Chris Vriend^{1,2} 

¹Amsterdam UMC, Vrije Universiteit Amsterdam, Department of Psychiatry, Amsterdam Neuroscience, De Boelelaan 1117, Amsterdam, Netherlands

²Amsterdam UMC, Vrije Universiteit Amsterdam, Department of Anatomy and Neurosciences, Amsterdam Neuroscience, De Boelelaan 1117, Amsterdam, Netherlands

Correspondence

Sophie M. D. D. Fitzsimmons, Department of Psychiatry, Amsterdam Neuroscience, Amsterdam UMC, Vrije Universiteit Amsterdam, Human and Life Sciences Building 13W55, De Boelelaan 1108, 1081 HZ Amsterdam, The Netherlands.
Email: s.fitzsimmons@amsterdamumc.nl

Funding information

Amsterdam Neuroscience; Nederlandse Organisatie voor Wetenschappelijk Onderzoek, Grant/Award Numbers: 91686036, 91717306

Abstract

Repetitive transcranial magnetic stimulation (rTMS) is used to investigate normal brain function in healthy participants and as a treatment for brain disorders. Various subject factors can influence individual response to rTMS, including brain network properties. A previous study by our group showed that “virtually lesioning” the left dorsolateral prefrontal cortex (dlPFC; important for cognitive flexibility) using 1 Hz rTMS reduced performance on a set-shifting task. We aimed to determine whether this behavioural response was related to topological features of pre-TMS resting-state and task-based functional networks. 1 Hz (inhibitory) rTMS was applied to the left dlPFC in 16 healthy participants, and to the vertex in 17 participants as a control condition. Participants performed a set-shifting task during fMRI at baseline and directly after a single rTMS session 1–2 weeks later. Functional network topology measures were calculated from resting-state and task-based fMRI scans using graph theoretical analysis. The dlPFC-stimulated group, but not the vertex group, showed reduced setshifting performance after rTMS, associated with lower task-based betweenness centrality (BC) of the dlPFC at baseline ($p = .030$) and a smaller reduction in task-based BC after rTMS ($p = .024$). Reduced repeat trial accuracy after rTMS was associated with higher baseline resting state node strength of the dlPFC ($p = .017$). Our results suggest that behavioural response to 1 Hz rTMS to the dlPFC is dependent on baseline functional network features. Individuals with more globally integrated stimulated regions show greater resilience to rTMS effects, while individuals with more locally well-connected regions show greater vulnerability.

KEYWORDS

cognition, dorsolateral prefrontal cortex, fMRI, graph analysis, network, set-shifting, transcranial magnetic stimulation

Abbreviations: BC, betweenness centrality; dlPFC, dorsolateral prefrontal cortex; FC, functional connectivity; HF, high frequency; LF, low frequency; MMSE, Mini Mental State Examination; NS, node strength; PC, participation coefficient; RER, repeat error rate; RRT, repeat reaction time; rTMS, repetitive transcranial magnetic stimulation; SER, shift error rate; SRT, shift reaction time.

This is an open access article under the terms of the Creative Commons Attribution-NonCommercial-NoDerivs License, which permits use and distribution in any medium, provided the original work is properly cited, the use is non-commercial and no modifications or adaptations are made.

© 2020 The Authors. *Human Brain Mapping* published by Wiley Periodicals, Inc.

1 | INTRODUCTION

Repetitive transcranial magnetic stimulation (rTMS) is a method of noninvasively exciting (using high frequency [HF] stimulation, >5 Hz) or inhibiting (using low frequency [LF] stimulation, ≤1 Hz) specific brain regions and connected networks through electromagnetic induction (Pell, Roth, & Zangen, 2011; Brückner, Kiefer, & Kammer, 2013). It is used to investigate brain function in healthy subjects (Luber & Lisanby, 2014) and is becoming a common treatment in neurological and psychiatric patient populations (Shafi, Westover, Fox, & Pascual-Leone, 2012). However, individuals vary considerably in their response to rTMS. This variation in response is associated with a number of factors, including baseline structural (Andoh, Matsushita, & Zatorre, 2015) and functional connectivity (FC) (Fox, Buckner, White, Greicius, & Pascual-Leone, 2012) of the stimulated brain network.

FC is a measure of the temporal correlation of activity between anatomically separate brain areas (Van Dijk et al., 2010). FC of the targeted area is predictive of the outcome of rTMS to the dorsolateral prefrontal cortex (dlPFC) for the treatment of depression (Bailey et al., 2018; Fox et al., 2012; Liston et al., 2014), dorsomedial PFC for the treatment of eating disorders (Dunlop et al., 2015), and of change in motor-evoked potential amplitude after rTMS of the motor cortex (Nettekoven et al., 2015). However, given that rTMS also influences the activity of areas distant to the stimulated site (Castrillon et al., 2020; van der Werf, Sanz-Arigita, Menning, & van den Heuvel, 2010), metrics that take the organisation of the wider functional network into account may be a more useful predictor of rTMS outcome than seed-based or region of interest (ROI)-based FC, which are limited to measuring FC between a priori-defined brain regions.

An alternative method is to define the brain as a network consisting of nodes (brain regions) and edges (functional connections between regions), and then apply graph theoretical analysis to evaluate the organisation and topology of this network (van den Heuvel & Hulshoff Pol, 2010). Graph measures can be extracted from the whole network, individual nodes, or subnetworks of more densely interconnected regions (also known as modules (Rubinov & Sporns, 2010)), allowing characteristics of the network to be evaluated at different spatial scales. While functional network features have been shown to be predictive of HF rTMS outcome in depression (Downar et al., 2014; Fan et al., 2019), and obsessive-compulsive disorder (Douw et al., 2019) this method has not yet been applied to the prediction of cognitive outcomes of LF rTMS.

In an earlier study by our group in healthy participants (Gerrits, van den Heuvel, & van der Werf, 2015), we applied LF rTMS to the left dlPFC, a region important for executive function, specifically the ability to flexibly adapt to changes in rules or environment (Mansouri, Tanaka, & Buckley, 2009; Niendam et al., 2012). Following rTMS, subjects showed a reduction in performance on a set-shifting task during fMRI. Set-shifting tests cognitive flexibility, or specifically the ability to flexibly switch between the rules used to complete a task—an ability that is associated with resilience to stress and is known to be impaired in psychiatric conditions such as obsessive-compulsive disorder and autism spectrum disorder (Dajani & Uddin, 2015). In the present reanalysis of resting-state and task-based fMRI data acquired

before and after rTMS, we aimed to determine whether baseline functional network characteristics are associated with behavioural response to inhibitory rTMS, and whether TMS-induced change in network characteristics is associated with change in performance.

We limited our choice of graph measures to those known to be markers of resilience and vulnerability to lesions, as we were investigating LF rTMS, which causes a temporary “virtual lesion.” *Centrality* (i.e., how well-connected a node is (Rubinov & Sporns, 2010)) is an important determinant of network resilience (Alstott, Breakspear, Hagmann, Cammoun, & Sporns, 2009). We applied three different centrality measures to the stimulated region: node strength (NS) which describes the total strength of a node's connections, and is considered to be an indicator of local connectivity; betweenness centrality (BC), which measures how many high strength paths in the network pass through a node; and participation coefficient (PC), which describes whether a node is connected mostly to its own module or to other modules (Rubinov & Sporns, 2010). Different types of centrality may have different implications for the rTMS-induced behavioural effects. Since the loss of highly locally connected nodes (such as those with high NS) is predictive of network disruption (Alstott et al., 2009; Warren et al., 2014), we predicted that this measure may be associated with greater vulnerability to the effects of inhibitory rTMS. On the other hand, nodes with high global connectivity (such as those with high BC or PC) are associated with greater cognitive flexibility (Cole, Yarkoni, Repovš, Anticevic, & Braver, 2012), suggesting that they may be resilient to cognitive disruption. Therefore, we expected that higher BC and PC of the stimulated node would be associated with higher resilience to inhibitory rTMS.

2 | METHODS

2.1 | Participants

Our sample consisted of 33 healthy participants originally recruited for a previous study (Gerrits, van der Werf, et al., 2015). Participants were not included if they suffered from neurological or psychiatric illnesses, substance abuse, cognitive deficits, or had a family history of epilepsy. Sixteen participants (mean age of 55 ± 9 years, nine men) were randomly appointed to dlPFC (verum) rTMS and 17 age and gender matched participants (mean age of 57 ± 10 years, 11 men) to vertex (active control) rTMS. All participants were screened for the presence of psychiatric disorders using the Structured Clinical Interview for DSM-IV Axis-I Disorders (Spitzer, Williams, Gibbon, & First, 1992), depressive symptoms using the Beck Depression Inventory (Beck, Steer, Ball, & Ranieri, 1996), anxiety symptoms using the Beck Anxiety Inventory (Beck, Epstein, Brown, & Steer, 1988), and general cognitive status using the Mini-Mental State Examination (MMSE) (Cockrell & Folstein, 1988). We used the Dutch version of the national adult reading test (Schmand, Bakker, Saan, & Louman, 1991) to provide an estimate of intelligence. The study protocol was reviewed and approved by the Research Ethics Committee of the VU University medical center (VUmc) and all participants provided written informed consent.

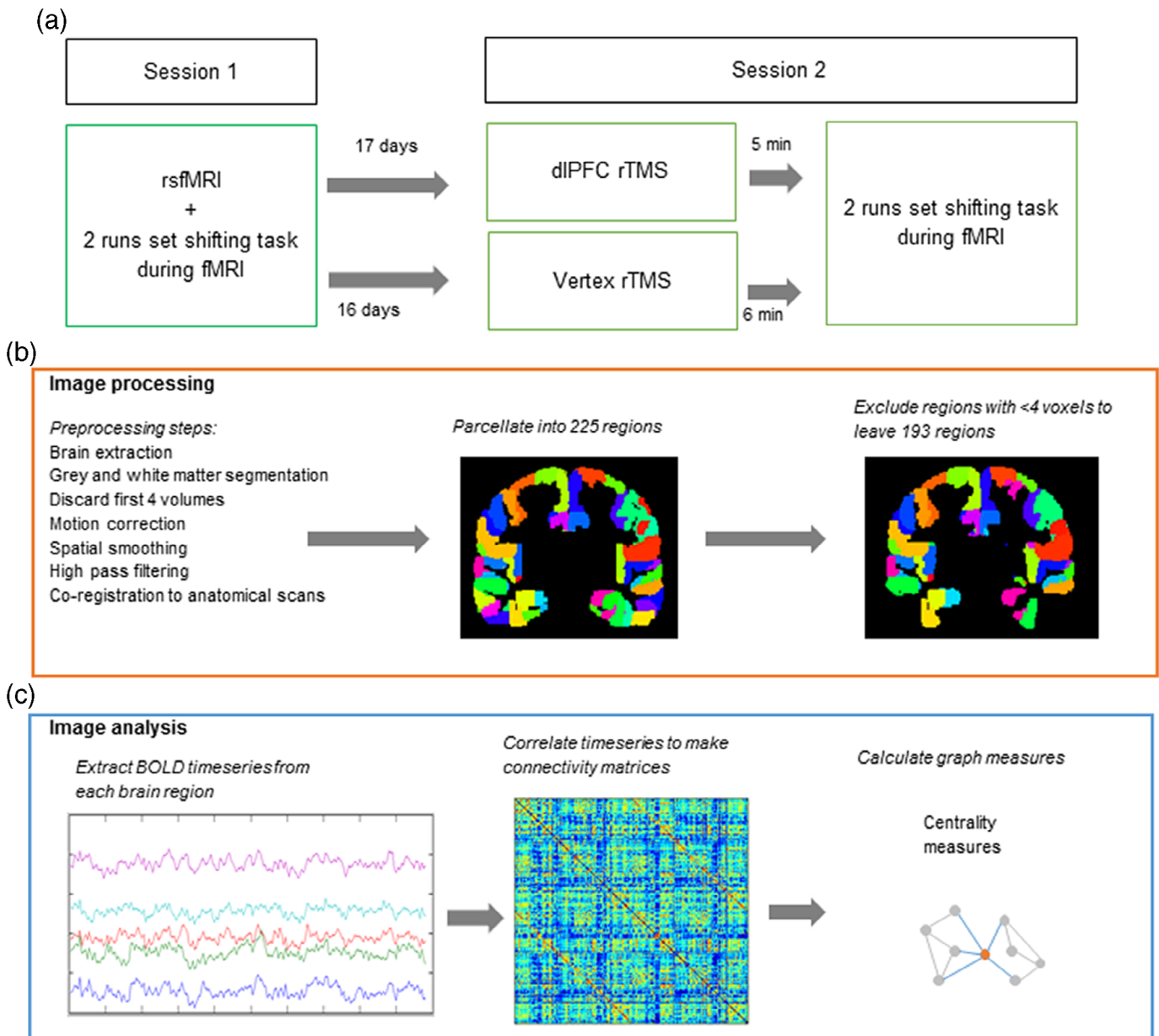


FIGURE 1 Study design and image processing/analysis. (a) Study design. All participants attended two sessions. During the first session, participants underwent an rsfMRI scan and carried out a set-shifting task during two separate runs of fMRI. Participants were then randomised to either verum (left dLPFC) or control (vertex) repetitive transcranial magnetic stimulation (rTMS) groups. After 16–17 days, participants attended the second session. They received rTMS, followed directly by carrying out the set-shifting task during two separate runs of fMRI. (b) Image processing steps: fMRI scans were preprocessed and parcellated into 225 regions. This was followed by exclusion of regions containing <4 voxels. (c) Image analysis steps: FC and graph theoretical analysis: The BOLD timeseries was extracted from each parcellated region. Pearson correlations were carried out between each pair of regions, giving a 193×193 correlation matrix for each participant. These matrices were then used to calculate centrality graph measures

2.2 | Experimental procedure

Full details of the experimental procedure and set-shifting task are reported in Gerrijs, van den Heuvel, et al. (2015). In brief, participants performed a set-shifting task during two fMRI sessions separated by an average of 16.9 ± 11.2 and 15.9 ± 7.7 days in the verum and control condition, respectively (Figure 1a). Participants received LF rTMS to either the dIPFC or vertex directly prior to the second fMRI session. For participants in the

verum group, fMRI data acquired during a set-shifting task in this first session were used to determine coordinates for TMS coil localisation using neuronavigation software (ASA4.1 software, ANT Neuro, The Netherlands). Specifically, the peak voxel of the switch>repeat contrast was used – individual coordinates were used per participant, but group mean MNI coordinates were $x = -42$, $y = 28$, $z = 31$ (see below for more details about the set-shifting task). For participants in the control condition, we used individual anatomical T1-weighted MR scans to determine the location of the

vertex (mean stimulated MNI coordinates $x = 0$, $y = -34$, $z = 70$). During the second session, 1 Hz rTMS was applied for 20 min (1,200 pulses total) using a hand-held figure-of-eight TMS coil (Medtronic MagOption, Medtronic Denmark A/S, Copenhagen, Denmark) at 110% of the individual motor threshold to “virtually lesion” the dlPFC or vertex. Participants then performed the set-shifting task for a second time during fMRI. The median interval between stimulation and the beginning of the set-shifting task was 5'19" for the verum and 5'56" for the control condition.

2.3 | Set-shifting task and behavioural data

During the set-shifting task (programmed in E-Prime version 2.0, Psychology Software Tools, Sharpsburg, PA), an arrow appeared either on one of four sides of a fixation cross in the centre of the screen, pointing either down, up, left, or right. The participant had to respond by pressing the up, down, left, or right key depending on whether the current classification rule for the arrow was *location* or *direction*. The participant was informed about incorrect repeat trials or a change in the classification rule (i.e., set-shift) by the presentation of a red screen. A green screen signalled a correct response. The task continued until the participant had completed 48 correct set shift trials, with a minimum of 15% correct trials. Two versions of the set-shifting task were counterbalanced between the first and second session that differed in the starting location and orientation of the arrow. All behavioural responses were recorded using an MRI compatible response box. The task was practiced prior to data collection to obtain a stable level of performance. Each response during the task was classified as correct repeat, incorrect repeat, successful shift, incorrect shift, or no shift/no repeat. Data from these responses (reaction time [RT] and error rate [ER]) were used to calculate the following behavioural outcome measures:

- Percentage change in repeat RT and shift RT (SRT) from baseline:

$$\frac{\text{RT Session 2} - \text{RT Session 1}}{\text{RT Session 1}} \times 100 = \% \text{change in RT}$$

- Percentage change in repeat ER (RER) and shift ER (SER) from baseline. A constant (c) was added to the ER of Session 1 when calculating percentage change to prevent dividing by zero:

$$\frac{\text{Failed trials per session}}{\text{Total trials per session}} = \text{ER per session}$$

$$\frac{\text{ER Session 2} - \text{ER Session 1}}{\text{ER Session 1} + c} \times 100 = \% \text{change in ER}$$

2.4 | Image acquisition

Functional imaging was performed at the VUmc, Amsterdam using a GE Signa HDxt 3-T MRI scanner (General Electric, Milwaukee, WI)

using whole-brain gradient echo-planar imaging (EPI) sequences. Eyes-closed rsfMRI images (TR 1,800 ms; TE = 30 ms; 64×64 matrix, flip angle = 80°), were acquired with 40 ascending slices per volume (3.75×3.75 mm in-plane resolution; slice thickness = 2.8 mm; inter-slice gap = 0.2 mm) and lasted 5.9 min in total (according to Van Dijk et al. (2010), connectivity estimates are stable within a 4-min timeseries). At baseline, rsfMRI scans were acquired before task-based scans. Functional images during the set-shifting task (TR = 2,100 ms; TE = 30 ms; 64×64 matrix, flip angle = 80°) with 40 ascending slices per volume (same resolution as rsfMRI) were acquired in two runs; runs varied in length between participants, as the set-shifting task lasted for as long as it took to achieve 48 correct set shifting trials. In the post-TMS task-based fMRI, the dlPFC group took on average 9.13 ± 0.95 min and 8.17 ± 0.39 min for the first and second runs, respectively. The control group 9.17 ± 0.70 and 8.16 ± 0.61 min. A sagittal 3D gradient-echo T1-weighted sequence (256×256 matrix; voxel size = $1 \times 0.977 \times 0.977$ mm; 172 sections) was also acquired for coregistration and parcellation.

2.5 | fMRI analysis

We chose to analyse the task-based scans as two separate runs in order to carry out a replication of our own analyses. Image processing of the two runs of the task scan and rsfMRI scan was performed using FMRIB's software library version 5.0.8 (FSL) (Smith et al., 2004) (Figure 1b) and included discarding the first four volumes of the functional scan to reach magnetization equilibrium, motion correlation, 5 mm spatial smoothing, and high-pass filtering (see Appendix A for more details). The brain was parcellated into 225 brain regions using 210 cortical regions from the Brainnetome atlas (Fan et al., 2016), 14 individually segmented subcortical areas and one cerebellar ROI from FSL's cerebellar atlas (Diedrichsen, Balsters, Flavell, Cussans, & Ramnani, 2009). To account for EPI distortions near air/tissue boundaries during scanning, we excluded any nodes with less than four signal containing voxels (Meijer et al., 2017). A total of 193 regions common to all fMRI runs remained: excluded regions were located in the orbitofrontal gyrus, inferior temporal gyrus, parahippocampal gyrus, and thalamus.

2.6 | Graph analyses

Connectivity analyses (Figure 1c) were performed using in-house scripts and the Brain Connectivity Toolbox (Rubinov & Sporns, 2010) in MATLAB R2012a (The MathWorks, Inc, Natick, MA). A connectivity matrix was created for each subject by calculating Pearson correlation coefficients between timeseries from all nodes. This was done separately for the RS scan and for each run of the task-based scans. The task-based scans were processed in one block without explicitly modelling the different task events (i.e., both repeat trials and switch trials were included in the task-based matrices). All weights in the connectivity matrix were absolutised. Using the absolute values prevents

loss of important interactions between brain regions (Fox et al., 2005) and using weighted rather than thresholded or binarised connectivity matrices avoids discarding weaker but potentially relevant connections (Knock et al., 2009). We carried out additional motion correction by “scrubbing” all time points with >0.5 mm of framewise displacement prior to making the correlation matrices (as recommended by Power, Barnes, Snyder, Schlaggar, and Petersen (2012)). Two participants had volumes flagged for scrubbing during resting state (one in the vertex condition, one in the DLPFC condition); a maximum of nine volumes were removed per participant (6% of total scan length, leaving 5.5 min of scan remaining). Thirteen participants had volumes flagged for scrubbing across the two baseline and two post-TMS task-based fMRI runs (six in the vertex condition, seven in the DLPFC condition); a maximum of 45 volumes were removed per participant per run (amounting to 17% of total scan length, leaving a minimum of 7.7 min of scan remaining).

Graph measures were calculated on a global and nodal scale. In order to identify the dIPFC node for each subject, we defined spherical ROIs (5 mm radius) corresponding to the coordinates of the stimulated brain area, and selected the atlas region that the ROI overlapped with most. An unstimulated node in the visual cortex (Node 202 from the Brainnetome Atlas, left V5) was also selected as a control node. We hypothesised that this node was unlikely to be affected by dIPFC rTMS, and was the node that appeared least frequently across individual participants' dIPFC-containing modules as calculated by Louvain modularity (see Appendix B for more details).

We calculated the following centrality graph measures in both groups for the dIPFC node and the control node in the visual cortex (Rubinov & Sporns, 2010):

- BC: The fraction of strongest weighted shortest paths that pass through a given node. This suggests that high BC nodes will be well connected throughout the entire network (Rubinov & Sporns, 2010).
- PC: An assessment of the type of connections a node has. Low PC indicates more high weighted connections with one's own module; high PC more high weighted connections to other modules (Sporns, 2014).
- NS: The sum of all edge weights, indicating how strongly connected a node is to its neighbours (Rubinov & Sporns, 2010).

2.7 | Statistical analyses

Statistical analyses were carried out in SPSS Statistics 22 (IBM Corp., Armonk, NY) and R. Independent samples *t* tests or Mann–Whitney *U* tests (two tailed, $\alpha = .05$) were used to compare demographic and behavioural characteristics of verum and control conditions, depending on the distribution. Since graph measures were not normally distributed, nonparametric tests were used for statistical analysis. Mann–Whitney *U* tests were used to compare baseline and rTMS-induced changes in graph measures between the verum and control groups. Correlations between graph measures and behavioural outcomes were carried out using Kendall's tau-b correlations with bootstrapped 95% confidence intervals (CIs). Due to high levels of

correlation between network measures and the exploratory nature of this study, these analyses were not corrected for multiple comparisons. The data did not meet the assumptions for regression analysis; therefore, to compare Kendall's tau coefficient between verum and control groups we converted Kendall's tau to Pearson's *r* using the formula $r = \sin(0.5 \pi \tau)$ (Walker, 2003) and calculated *z* scores using a Fisher's *r*-to-*Z* transform (Diedenhofen & Musch, 2015).

3 | RESULTS

3.1 | Demographic characteristics and session information

The verum and control groups were well matched in terms of age ($p = .606$), sex ($p = .619$), and MMSE ($p = .360$), but the control group had a higher estimated intelligence ($p = .012$) (Table 1). The interval between Sessions 1 and 2 ($p = .930$) and between rTMS and task ($p = .053$) did not differ significantly between groups (Table 1).

3.2 | Change in set shifting performance after rTMS

Groups did not differ in set shifting performance at baseline (Gerrits, van den Heuvel, et al., 2015) (see also Appendix C, Table S1). There was a small rTMS-induced increase in SER in the verum group compared with the control group ($p = .049$, Table 1). There were no other significant between-group differences in rTMS induced changes in set shifting performance. For both groups there was, in general, an improvement in performance between Sessions 1 and 2 in all behavioural measures except for SER. None of the changes in behavioural outcomes correlated with intelligence, educational level, MMSE, or rTMS-task interval (see Appendix C, Table S2).

3.3 | Association of behaviour change after rTMS with baseline resting state graph measures

The verum and control groups did not differ significantly in any resting state graph measures at baseline (see Appendix C, Table S3). In the verum group, there was a positive correlation between the change in (Δ RER and baseline NS of the dIPFC node ($\tau = 0.447$, $p = .017$, 95% CI [0.138, 0.781]) (Figure 2a)—that is, the higher the prestimulation NS, the greater the increase in repeat errors after rTMS. This association was not seen in the control group ($\tau = -0.170$, $p = .343$, 95% CI [-0.527, 0.214]), and the association in the verum group was also significantly stronger than that seen in the control group ($z = 2.696$, $p = .007$). In the verum group, there was no significant association between NS in the control node within the visual cortex and Δ RER ($\tau = 0.380$, 95% CI [-0.049, 0.698]). None of the other resting state graph measures examined (BC and PC) showed significant correlations with change in cognitive performance (see Appendix C, Table S4).

TABLE 1 Demographic characteristics, session information and change in set shifting performance after rTMS

| | Verum group <i>n</i> = 16 | Control group <i>n</i> = 17 | <i>p</i> |
|---|------------------------------|------------------------------|-------------------|
| <i>Demographics</i> | | | |
| Age (years) | 55 ± 9 (39–75) | 57 ± 10 (41–70) | .606 ^a |
| Sex (no./% men) | 9/56% | 11/65% | .619 ^b |
| Level of education reached ^c (median, range, % >5) | 6 (4–7) 69% | 6 (3–7) 59% | .721 ^b |
| Estimated IQ | 98 ± 12 (73–123) | 110 ± 14 (82–130) | .012 |
| MMSE | 29 ± 1 (28–30) | 29 ± 1 (27–30) | .360 |
| <i>Session information</i> | | | |
| Interval Session 1–Session 2 (days) | 17 ± 11 (7–56) | 16 ± 8 (7–35) | .772 ^a |
| Interval rTMS–task (s) | 319 ± 54 (240–488) | 356 ± 137 (277–800) | .053 |
| Total trials completed Day 1 | 276.6 ± 6.8 (263–289) | 278.4 ± 10.9 (263–299) | .578 ^a |
| Total trials completed Day 2 | 274.6 ± 5.6 (265–288) | 280.0 ± 9.4 (264–298) | .054 ^a |
| <i>Change in set shifting performance after rTMS (% change from baseline)</i> | | | |
| RRT | −2.44 ± 14.70 (−30.65–33.41) | −6.00 ± 17.72 (−30.47–27.40) | .488 |
| SRT | −5.08 ± 8.01 (−21.75–14.36) | −9.17 ± 15.59 (−38.93–18.95) | .465 |
| RER | −0.26 ± 0.54 (−1.50–0.73) | −0.06 ± 0.65 (−1.09–1.67) | .533 |
| SER | 0.43 ± 0.96 (−1.13–3.12) | −0.27 ± 1.05 (−2.56–1.37) | .049 |

Note: Values are presented as mean ± SD (range) unless otherwise indicated. Significance of group differences tested using an independent samples Mann–Whitney *U* test unless otherwise indicated.

Abbreviations: MMSE, Mini-Mental State Examination; RRT, repeat response time; SRT, switch response time; RER, repeat error rate; rTMS, Repetitive transcranial magnetic stimulation; SER, switch error rate.

^aIndependent samples *t* test.

^bPearson's χ^2 test.

^cLevel of education expressed as the Verhage 7-point scale (Verhage, 1964): 1 = no finished education; 5 = secondary school, medium level; 7 = university training. Proportions of people scoring ≤5 and >5 compared using χ^2 test.

3.4 | Association of behaviour change after rTMS with baseline task-based graph measures

In the verum group, BC of the dlPFC node correlated negatively with percentage change in shift response time (Δ SRT) for both the first ($\tau = -0.403$, $p = .030$, 95% CI [−0.733, −0.031]) and second run of task-based fMRI ($\tau = -0.367$, $p = .048$, 95% CI [−.692, 0]) (Figure 2b); that is, the lower the BC, the greater the increase in shift response time after rTMS. This relationship was not seen for BC of the dlPFC in the control group ($\tau = -0.067$, $p = .710$, 95% CI [−0.327, 0.267]) or for the BC of the control node of the verum group ($\tau = -0.017$, $p = .928$, 95% CI [−0.482, 0.440]). The correlation in the verum group was also significantly stronger than that of the control group ($z = -2.040$, $p = .04$). Correlations between other task-based graph measures (NS and PC) and changes in behaviour were not significant (see Appendix C, Table S6).

3.5 | Change in task-based graph measures after rTMS

There was no significant difference between verum and control groups in terms of change in network topology after rTMS in either the first or second run of task-based fMRI (see Appendix C, Table S7).

3.6 | Association of change in behaviour with change in task-based graph measures

In the verum group, percentage change in Δ SER between sessions was positively correlated with change in BC (Δ BC) of the dlPFC node, but only for the second run ($\tau = 0.424$, $p = .024$, 95% CI [0.150, 0.669]) (Figure 3). In other words, subjects showing an rTMS-induced decrease in BC also had a decreased SER after rTMS. Conversely, those with no change or an increase in BC had an increased SER. There was no significant correlation between Δ SER and Δ BC in the control group ($\tau = -0.180$, $p = .319$, 95% CI: [−0.454, 0.129]) and there was no correlation with Δ BC of the control node ($\tau = -0.059$, $p = .752$, 95% CI: [−0.581, 0.415]). Furthermore, the correlation coefficients differed significantly between groups ($z = 2.617$, $p = 0.008$). There was no other significant correlation between changes in task-based graph measures (NS, PC) and changes in behaviour (see Appendix C, Table S8).

4 | DISCUSSION

We investigated whether functional network topology of prestimulation rsfMRI or task-based fMRI was associated with the change in set-shifting performance after inhibitory rTMS to the dlPFC, and whether this change was also related to change in graph features

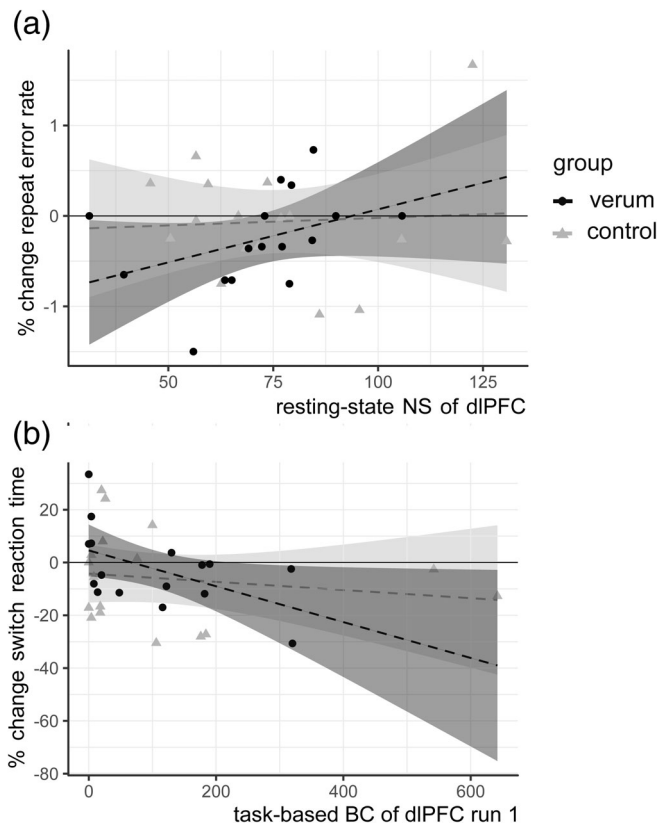


FIGURE 2 Correlations between baseline fMRI graph measures and change in cognitive performance after low frequency (LF) repetitive transcranial magnetic stimulation (rTMS): (a) Higher resting state node strength (NS) of the left dorsolateral prefrontal cortex (dlPFC) node is associated with an increase in RER in the verum group ($\tau = 0.447$, $p = .017$, 95% CI [0.138, 0.781]) but not in the control group ($\tau = -0.170$, $p = .343$, 95% CI [-0.527, 0.214]; $z = 2.696$, $p = 0.007$). (b) Lower betweenness centrality (BC) of the dlPFC node is associated with an increase in SRT in the verum group after TMS ($\tau = -0.403$, $p = .03$, 95% CI [-0.733, -0.031]) but not in the control group ($\tau = -0.067$, $p = .710$, 95% CI [-0.327, 0.267]; $z = -2.040$, $p = 0.04$). Shaded areas on plot correspond to (linear) 95% CIs. Note that a linear correlation line and 95% CIs are drawn in these figures, but this association was tested nonparametrically

after stimulation. Our findings indicate that individuals with a higher pre-TMS BC of the dlPFC during set-shifting are less affected by inhibitory rTMS, and also show a large decrease in task-based BC following rTMS. Additionally, individuals with a higher pre-TMS NS of the dlPFC during resting state are more affected by inhibitory rTMS.

4.1 | Functional network topology and response to LF rTMS

BC gives an indication of the level of global integration of a node. In our study, the detrimental effect of LF rTMS was greater in subjects with a lower pre-TMS BC of the dlPFC (i.e., a more segregated dlPFC), resulting in a post-rTMS increase in SRT. Conversely, subjects with a higher BC of the dlPFC (i.e., a more integrated dlPFC) appeared to be

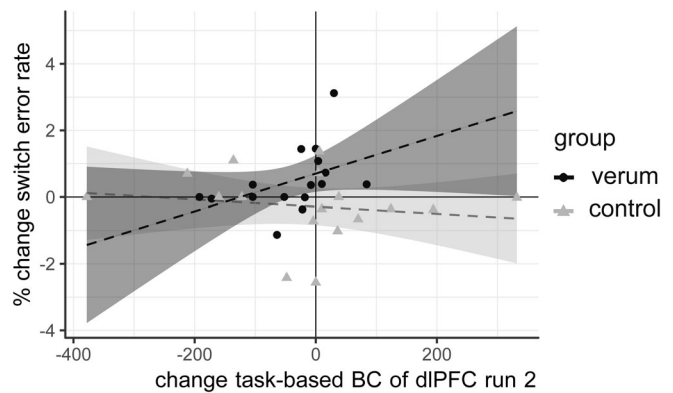


FIGURE 3 Change in task-based betweenness centrality (BC) of the left dorsolateral prefrontal cortex (dlPFC) after repetitive transcranial magnetic stimulation (rTMS) is associated with change in shift error rate after rTMS: Participants with no change in task-based BC of the dlPFC after rTMS showed an increase in shift errors, while participants with a decrease in BC after rTMS was showed an improvement or no change in shift errors (verum group: $\tau = 0.424$, $p = .024$, 95% CI [0.150, 0.669]; control group: $\tau = -0.180$, $p = .319$, 95% CI [-0.454, 0.129], $z = 2.617$, $p = .008$). Shaded areas on plot correspond to 95% CIs. Note that a linear correlation line and 95% CIs are drawn in these figures, but this association was tested nonparametrically

less affected and showed post-rTMS improvement in SRT. Other studies examining network topology predictors of rTMS effect have also found evidence for a greater effect with less integration. The effect of 10 Hz dlPFC rTMS in depression (Fan et al., 2019) and obsessive-compulsive disorder (Douw et al., 2019) is greater with a more segregated salience network and a less promiscuous stimulated region, respectively. This suggests that when applied to less well-integrated brain areas, rTMS effects may be restricted to the local region and therefore have a stronger effect on the specific function of that region. We also found that subjects whose behavioural performance was least affected by the LF rTMS not only had a higher baseline BC of the dlPFC, but also showed the greatest rTMS-induced decrease in BC. This suggests that the capacity to "lose" BC and thereby buffer the effects of LF rTMS may be a possible mechanism of resilience to inhibitory rTMS. This apparent resilience of globally well-integrated nodes to inhibition may only be true in the case of inhibitory rTMS, where brain excitability is temporarily reduced rather than blocked completely: a computational lesion study showed that full deletion of nodes with high BC resulted in global network dysfunction (Alstott et al., 2009).

We also found an association between higher resting state NS of the dlPFC and rTMS-induced increase in repeat errors. This implies that regions with a higher NS are more vulnerable to the inhibitory effects of rTMS. As NS is a measure of the strength of the connections of a node with its neighbours (Rubinov & Sporns, 2010), their loss may lead to network dysfunction (Alstott et al., 2009). Previous seed-based FC fMRI studies also suggest that the effectiveness of rTMS is dependent on the strength of the connections of the stimulated site; stimulation of regions that have a greater FC at baseline (Cárdenas-Morales et al., 2014; Liston et al., 2014) results in a greater rTMS response.

Inhibitory rTMS may therefore be more effective in subjects with a high baseline resting NS because it allows the effects of inhibition to spread more easily to functionally connected regions. This effect is not limited to LF rTMS: A study of network features predicting HF rTMS effects in patients with obsessive-compulsive disorder also found that higher NS of the stimulated network predicted greater distress reduction following rTMS (Douw et al., 2019).

4.2 | Differences between resting state and task-based graph measures

Interestingly, although resting state and task-based networks are similar in structure (Smith et al. 2009), different graph measures were associated with a reduction in different aspects of behavioural performance during set-shifting after rTMS in task-based and rsfMRI. BC and Δ BC in task-based scans were specifically associated with change in set shifting performance, while NS in resting state scans was associated with errors on repeat trials. The prominence of BC in the task-based fMRI and NS in rsfMRI could be due to the changes in functional network topology that take place when transitioning from rest to task states. The brain network is more integrated during task execution (with higher BC of the relevant nodes) (Bolt, Laurienti, Lyday, Morgan, & Dagenbach, 2016; Kitzbichler, Henson, Smith, Nathan, & Bullmore, 2011; Rzucidlo, Roseman, Laurienti, & Dagenbach, 2013) while measures related to NS are more important during rest (Bolt et al., 2016; Rzucidlo et al., 2013). The specific prediction of switch trial performance by the task-based network and repeat trials by the resting state network could be explained by the association of these networks with the different cognitive aspects of the task. The task-based network predicts the effect of disruption of the brain region (i.e., DLPFC) associated with that specific task (i.e., set shifting). Repeat trials, where subjects respond to the direction or position of an arrow rather than switching between response rules, involve more general, fundamental cognitive abilities, such as working memory and attention (Braver et al., 2003; Monsell, 2003). The impairment of these cognitive domains is, in our study, predicted by the resting state network (the topology of which has been previously associated with fundamental cognitive skills such as working memory (Cole et al., 2012) Network measures derived from task-based fMRI may therefore have more specificity for predicting rTMS-induced behavioural changes on the same task. However, the fact that RSfMRI can also predict rTMS effects has practical implications: RSfMRI allows evaluation of multiple cortical systems within a single session, is more reproducible between sites, and less dependent on participant factors than task-based fMRI (Fox & Greicius, 2010; Leuthardt et al., 2018), and may therefore be more feasible to use in future clinical trials and other clinical contexts as a predictor of rTMS outcomes.

4.3 | Limitations and strengths

Our exploratory study has some limitations. First, the relatively small sample size means that our power is limited and any effects present may be inflated (Yarkoni, 2009). Second, the rTMS-induced

performance changes are subtle. Tasks with higher cognitive loads or stronger rTMS stimulation may give larger and more robust effects. Third, the interval between pre-rTMS scan and the actual day of rTMS was approximately 2 weeks—it is unknown how representative the networks measured at Session 1 were of the prestimulation networks actually present at Session 2 (though FC measures have been shown to stay largely stable over time (Gratton et al., 2018; Laumann et al., 2015). Our cohort also has a wide age range (39–75) and an average age of 56. This may mean that our results are less applicable to younger age groups as graph features have been shown to vary with age (Jordan et al., 2018) (though graph measures showed no correlation with age in our sample [Appendix C, Table S9]). Finally, since we did not objectively monitor the wakefulness of the subjects during the resting state scan (which can affect connectivity measures, see Tagliazucchi & Laufs 2014), we cannot exclude possible differences in vigilance between the vertex and DLPFC groups. Replication of this study in a larger cohort with a more demanding task could help tackle these problems. Our study also has a number of strengths. The association of low baseline task-based BC with increase in switch response time was reproduced in the second run of task-based fMRI. The observed effects also survive strict “scrubbing” motion correction.

4.4 | Implications and future work

Our results have implications for the selection of rTMS targets. Baseline functional network topology may be an important factor to consider when choosing stimulation targets for therapies involving LF rTMS (e.g., in the treatment of obsessive-compulsive disorder, stroke, and auditory hallucinations (Shafi et al., 2012) or in the experimental modelling of the cognitive deficits seen in these diseases in healthy controls. Given that our study was carried out in healthy controls, we cannot comment directly on the utility of this finding in a clinical context. However, a similar analysis in a group of OCD patients (Douw et al., 2019) showed comparable results (that low integration and high segregation of the stimulated region predict a greater effect of rTMS), suggesting that this finding may also be applicable in patient populations. Future work could explore whether the effects demonstrated in this exploratory study are consistent across other stimulation sites, for other cognitive tasks, or for clinical improvement in disease states across multiple sessions; which graph measures or combination of graph measures are the best predictors of rTMS effect; which graph measures predict the outcome of excitatory rTMS; and whether specifically targeting nodes with high NS or low BC results in more consistent rTMS outcome.

5 | CONCLUSIONS

We have shown that changes in cognitive performance after inhibitory rTMS to the dlPFC are associated with baseline resting state and task-based functional network graph measures. Subjects with stimulated regions that are globally well-connected during a task are more

resilient to the effects of inhibitory rTMS, while those with stimulated regions with strong local connections in the resting state are more vulnerable to inhibitory rTMS. These results have important implications for our understanding of individual variability in response to rTMS, and for the practical application of this noninvasive brain stimulation technique.

ACKNOWLEDGMENTS

The authors would like to thank Dr Niels Gerrits for his help with data collection and Prof Dr Jos Twisk for advice on statistical analysis. This work was supported by a grant from Amsterdam Neuroscience, a NWO-ZonMw VENI grant (91686036) and a NWO-ZonMw VIDI grant (91717306) (both awarded to O. A. van den H.).

CONFLICT OF INTEREST

The authors declare no potential conflict of interest.

DATA AVAILABILITY STATEMENT

Data availability statement: The data that support the findings of this study are available from the corresponding author upon reasonable request.

ORCID

Sophie M. D. D. Fitzsimmons  <https://orcid.org/0000-0002-7216-4958>

Chris Vriend  <https://orcid.org/0000-0003-3111-1304>

REFERENCES

- Alstott, J., Breakspear, M., Hagmann, P., Cammoun, L., & Sporns, O. (2009). Modeling the impact of lesions in the human brain. *PLoS Computational Biology*, 5(6), e1000408. <https://doi.org/10.1371/journal.pcbi.1000408>
- Andoh, J., Matsushita, R., & Zatorre, R. J. (2015). Asymmetric inter-hemispheric transfer in the auditory network: Evidence from TMS, resting-state fMRI, and diffusion imaging. *Journal of Neuroscience*, 35(43), 14602–14611. <https://doi.org/10.1523/JNEUROSCI.2333-15.2015>
- Bailey, N. W., Hoy, K. E., Rogasch, N. C., Thomson, R. H., McQueen, S., Elliot, D., ... Fitzgerald, P. B. (2018). Differentiating responders and non-responders to rTMS treatment for depression after one week using resting EEG connectivity measures. *Journal of Affective Disorders*, 242, 68–79. <https://doi.org/10.1016/j.jad.2018.08.058>
- Beck, A. T., Epstein, N., Brown, G., & Steer, R. A. (1988). An inventory for measuring clinical anxiety: Psychometric properties. *Journal of Consulting and Clinical Psychology*, 56(6), 893–897.
- Beck, A. T., Steer, R. A., Ball, R., & Ranieri, W. (1996). Comparison of Beck Depression Inventories -IA and -II in psychiatric outpatients. *Journal of Personality Assessment*, 67(3), 588–597. https://doi.org/10.1207/s15327752jpa6703_13
- Beckmann, C. F., DeLuca, M., Devlin, J. T., & Smith, S. M. (2005). Investigations into resting-state connectivity using independent component analysis. *Philosophical Transactions of the Royal Society of London Series B, Biological Sciences*, 360(1457), 1001–1013 <https://doi.org/10.1098/rstb.2005.1634>
- Bolt, T., Laurienti, P. J., Lyday, R., Morgan, A., & Dagenbach, D. (2016). Graph-theoretical study of functional changes associated with the Iowa gambling task. *Frontiers in Human Neuroscience*, 10, 314. <https://doi.org/10.3389/fnhum.2016.00314>
- Braver, T. S., Reynolds, J. R., & Donaldson, D. I. (2003). Neural mechanisms of transient and sustained cognitive control during task switching. *Neuron*, 39(4), 713–726. [https://doi.org/10.1016/S0896-6273\(03\)00466-5](https://doi.org/10.1016/S0896-6273(03)00466-5)
- Brückner, S., Kiefer, M., & Kammer, T. (2013). Comparing the after-effects of continuous theta burst stimulation and conventional 1Hz rTMS on semantic processing. *Neuroscience*, 233, 64–71. <https://doi.org/10.1016/j.neuroscience.2012.12.033>
- Cárdenas-Morales, L., Volz, L. J., Michely, J., Rehme, A. K., Pool, E.-M., Nettekoven, C., ... Grefkes, C. (2014). Network connectivity and individual responses to brain stimulation in the human motor system. *Cerebral Cortex*, 24(7), 1697–1707. <https://doi.org/10.1093/cercor/bht023>
- Castrillon, G., Sollmann, N., Kurcyus, K., Razi, A., Krieg, S. M., & Riedel, V. (2020). The physiological effects of noninvasive brain stimulation fundamentally differ across the human cortex. *Science Advances*, 6(5), eaay2739. <https://doi.org/10.1126/sciadv.aay2739>
- Cockrell, J. R., & Folstein, M. F. (1988). Mini-mental state examination (MMSE). *Psychopharmacology Bulletin*, 24(4), 689–692.
- Cole, M. W., Yarkoni, T., Repovš, G., Anticevic, A., & Braver, T. S. (2012). Global connectivity of prefrontal cortex predicts cognitive control and intelligence. *Journal of Neuroscience*, 32(26), 8988–8999. <https://doi.org/10.1523/JNEUROSCI.0536-12.2012>
- Dajani, D. R., & Uddin, L. Q. (2015). Demystifying cognitive flexibility: Implications for clinical and developmental neuroscience. *Trends in Neurosciences*, 38(9), 571–578. <https://doi.org/10.1016/j.tins.2015.07.003>
- DeSalvo, M. N., Douw, L., Takaya, S., Liu, H., & Stufflebeam, S. M. (2014). Task-dependent reorganisation of functional connectivity networks during visual semantic decision making. *Brain and Behavior*, 4(6), 877–885. <https://doi.org/10.1002/brb3.286>
- Diedenhofen, B., & Musch, J. (2015). Cocor: A comprehensive solution for the statistical comparison of correlations. *PLoS One*, 10(4), e0121945. <https://doi.org/10.1371/journal.pone.0121945>
- Diedrichsen, J., Balsters, J. H., Flavell, J., Cussans, E., & Ramnani, N. (2009). A probabilistic MR atlas of the human cerebellum. *NeuroImage*, 46(1), 39–46. <https://doi.org/10.1016/j.neuroimage.2009.01.045>
- Doron, K. W., Bassett, D. S., & Gazzaniga, M. S. (2012). Dynamic network structure of interhemispheric coordination. *Proceedings of the National Academy of Sciences of the United States of America*, 109(46), 18661–18668 <https://doi.org/10.1073/pnas.1216402109>
- Douw, L., Quaak, M., Fitzsimmons, S. M. D. D., de Wit, S. J., van der Werf, Y. D., van den Heuvel, O. A., & Vriend, C. (2019). Static and dynamic network properties of the repetitive transcranial magnetic stimulation target predict changes in emotion regulation in obsessive-compulsive disorder. *Brain Stimulation*, 13, 318–326. <https://doi.org/10.1016/j.brs.2019.10.017>
- Downar, J., Geraci, J., Salomons, T. V., Dunlop, K., Wheeler, S., McAndrews, M. P., ... Giacobbe, P. (2014). Anhedonia and reward-circuit connectivity distinguish nonresponders from responders to dorsomedial prefrontal repetitive transcranial magnetic stimulation in major depression. *Biological Psychiatry*, 76(3), 176–185. <https://doi.org/10.1016/j.biopsych.2013.10.026>
- Dunlop, K., Woodside, B., Lam, E., Olmsted, M., Colton, P., Giacobbe, P., & Downar, J. (2015). Increases in frontostriatal connectivity are associated with response to dorsomedial repetitive transcranial magnetic stimulation in refractory binge/purge behaviors. *NeuroImage: Clinical*, 8, 611–618. <https://doi.org/10.1016/j.nicl.2015.06.008>
- Fan, J., Tso, I. F., Maixner, D. F., Abagis, T., Hernandez-Garcia, L., & Taylor, S. F. (2019). Segregation of salience network predicts treatment response of depression to repetitive transcranial magnetic stimulation. *NeuroImage: Clinical*, 22, 101719. <https://doi.org/10.1016/j.nicl.2019.101719>
- Fan, L., Li, H., Zhuo, J., Zhang, Y., Wang, J., Chen, L., ... Jiang, T. (2016). The human Brainnetome atlas: A new brain atlas based on connectonal

- architecture. *Cerebral Cortex*, 26(8), 3508–3526. <https://doi.org/10.1093/cercor/bhw157>
- Fox, M. D., Buckner, R. L., White, M. P., Greicius, M. D., & Pascual-Leone, A. (2012). Efficacy of transcranial magnetic stimulation targets for depression is related to intrinsic functional connectivity with the subgenual cingulate. *Biological Psychiatry*, 72(7), 595–603. <https://doi.org/10.1016/j.biopsych.2012.04.028>
- Fox, M. D., & Greicius, M. (2010). Clinical applications of resting state functional connectivity. *Frontiers in Systems Neuroscience*, 4, 19. <https://doi.org/10.3389/fnsys.2010.00019>
- Fox, M. D., Snyder, A. Z., Vincent, J. L., Corbetta, M., Essen, D. C. V., & Raichle, M. E. (2005). The human brain is intrinsically organized into dynamic, anticorrelated functional networks. *Proceedings of the National Academy of Sciences of the United States of America*, 102(27), 9673–9678. <https://doi.org/10.1073/pnas.0504136102>
- Gerrits, N. J. H. M., van den Heuvel, O. A., & van der Werf, Y. D. (2015). Decreased neural activity and neural connectivity while performing a set-shifting task after inhibiting repetitive transcranial magnetic stimulation on the left dorsal prefrontal cortex. *BMC Neuroscience*, 16, 45. <https://doi.org/10.1186/s12868-015-0181-3>
- Gerrits, N. J. H. M., van der Werf, Y. D., Verhoef, K. M. W., Veltman, D. J., Groenewegen, H. J., Berendse, H. W., & van den Heuvel, O. A. (2015). Compensatory fronto-parietal hyperactivation during set-shifting in unmedicated patients with Parkinson's disease. *Neuropsychologia*, 68, 107–116. <https://doi.org/10.1016/j.neuropsychologia.2014.12.022>
- Gratton, C., Laumann, T. O., Nielsen, A. N., Greene, D. J., Gordon, E. M., Gilmore, A. W., ... Petersen, S. E. (2018). Functional brain networks are dominated by stable group and individual factors, not cognitive or daily variation. *Neuron*, 98(2), 439–452.e5. <https://doi.org/10.1016/j.neuron.2018.03.035>
- Jenkinson, M., Bannister, P., Brady, M., & Smith, S. (2002). Improved optimization for the robust and accurate linear registration and motion correction of brain images. *NeuroImage*, 17(2), 825–841.
- Kitzbichler, M. G., Henson, R. N. A., Smith, M. L., Nathan, P. J., & Bullmore, E. T. (2011). Cognitive effort drives workspace configuration of human brain functional networks. *The Journal of Neuroscience: The Official Journal of the Society for Neuroscience*, 31(22), 8259–8270. <https://doi.org/10.1523/JNEUROSCI.0440-11.2011>
- Knock, S. A., McIntosh, A. R., Sporns, O., Kötter, R., Hagmann, P., & Jirsa, V. K. (2009). The effects of physiologically plausible connectivity structure on local and global dynamics in large scale brain models. *Journal of Neuroscience Methods*, 183(1), 86–94. <https://doi.org/10.1016/j.jneumeth.2009.07.007>
- Lancichinetti, A., & Fortunato, S. (2012). Consensus clustering in complex networks. *Scientific Reports*, 2, 336. <https://doi.org/10.1038/srep00336>
- Laumann, T. O., Gordon, E. M., Adeyemo, B., Snyder, A. Z., Joo, S. J., Chen, M.-Y., ... Petersen, S. E. (2015). Functional system and areal organization of a highly sampled individual human brain. *Neuron*, 87(3), 657–670. <https://doi.org/10.1016/j.neuron.2015.06.037>
- Leuthardt, E. C., Guzman, G., Bandt, S. K., Hacker, C., Vellimana, A. K., Limbrick, D., ... Benzinger, T. L. S. (2018). Integration of resting state functional MRI into clinical practice—A large single institution experience. *PLoS One*, 13(6), e0198349. <https://doi.org/10.1371/journal.pone.0198349>
- Liston, C., Chen, A. C., Zebley, B. D., Drysdale, A. T., Gordon, R., Leuchter, B., ... Dubin, M. J. (2014). Default mode network mechanisms of transcranial magnetic stimulation in depression. *Biological Psychiatry*, 76(7), 517–526. <https://doi.org/10.1016/j.biopsych.2014.01.023>
- Lordan, A. D., Cooke, K. A., Moored, K. D., Katz, B., Buschkuhl, M., Jaeggi, S. M., ... Reuter-Lorenz, P. A. (2018). Aging and network properties: Stability over time and links with learning during working memory training. *Frontiers in Aging Neuroscience*, 9, 419. <https://doi.org/10.3389/fnagi.2017.00419>
- Luber, B., & Lisanby, S. H. (2014). Enhancement of human cognitive performance using transcranial magnetic stimulation (TMS). *NeuroImage*, 85(03), 961–970. <https://doi.org/10.1016/j.neuroimage.2013.06.007>
- Mansouri, F. A., Tanaka, K., & Buckley, M. J. (2009). Conflict-induced behavioural adjustment: A clue to the executive functions of the prefrontal cortex. *Nature Reviews Neuroscience*, 10(2), 141–152. <https://doi.org/10.1038/nrn2538>
- Meijer, K. A., Eijlers, A. J. C., Douw, L., Uitdehaag, B. M. J., Barkhof, F., Geurts, J. J. G., & Schoonheim, M. M. (2017). Increased connectivity of hub networks and cognitive impairment in multiple sclerosis. *Neurology*, 88(22), 2107–2114. <https://doi.org/10.1212/WNL.0000000000003982>
- Monsell, S. (2003). Task switching. *Trends in Cognitive Sciences*, 7(3), 134–140. [https://doi.org/10.1016/S1364-6613\(03\)00028-7](https://doi.org/10.1016/S1364-6613(03)00028-7)
- Nettekoven, C., Volz, L. J., Leimbach, M., Pool, E.-M., Rehme, A. K., Eickhoff, S. B., ... Grefkes, C. (2015). Inter-individual variability in cortical excitability and motor network connectivity following multiple blocks of rTMS. *NeuroImage*, 118, 209–218. <https://doi.org/10.1016/j.neuroimage.2015.06.004>
- Niendam, T. A., Laird, A. R., Ray, K. L., Dean, Y. M., Glahn, D. C., & Carter, C. S. (2012). Meta-analytic evidence for a superordinate cognitive control network subserving diverse executive functions. *Cognitive, Affective, & Behavioral Neuroscience*, 12(2), 241–268. <https://doi.org/10.3758/s13415-011-0083-5>
- Patenaude, B., Smith, S. M., Kennedy, D. N., & Jenkinson, M. (2011). A Bayesian model of shape and appearance for subcortical brain segmentation. *NeuroImage*, 56(3), 907–922. <https://doi.org/10.1016/j.neuroimage.2011.02.046>
- Pell, G. S., Roth, Y., & Zangen, A. (2011). Modulation of cortical excitability induced by repetitive transcranial magnetic stimulation: Influence of timing and geometrical parameters and underlying mechanisms. *Progress in Neurobiology*, 93(1), 59–98. <https://doi.org/10.1016/j.pneurobio.2010.10.003>
- Power, J. D., Barnes, K. A., Snyder, A. Z., Schlaggar, B. L., & Petersen, S. E. (2012). Spurious but systematic correlations in functional connectivity MRI networks arise from subject motion. *NeuroImage*, 59(3), 2142–2154. <https://doi.org/10.1016/j.neuroimage.2011.10.018>
- Rubinov, M., & Sporns, O. (2010). Complex network measures of brain connectivity: Uses and interpretations. *NeuroImage*, 52(3), 1059–1069. <https://doi.org/10.1016/j.neuroimage.2009.10.003>
- Rzucidlo, J. K., Roseman, P. L., Laurienti, P. J., & Dagenbach, D. (2013). Stability of whole brain and regional network topology within and between resting and cognitive states. *PLoS One*, 8(8), e70275. <https://doi.org/10.1371/journal.pone.0070275>
- Schmand, B., Bakker, D., Saan, R., & Louman, J. (1991). The Dutch reading test for adults: A measure of premorbid intelligence level. *Tijdschrift voor Gerontologie en Geriatrie*, 22(1), 15–19.
- Shafi, M. M., Westover, M. B., Fox, M. D., & Pascual-Leone, A. (2012). Exploration and modulation of brain network interactions with noninvasive brain stimulation in combination with neuroimaging. *The European Journal of Neuroscience*, 35(6), 805–825. <https://doi.org/10.1111/j.1460-9568.2012.08035.x>
- Smith, S. M. (2002). Fast robust automated brain extraction. *Human Brain Mapping*, 17(3), 143–155. <https://doi.org/10.1002/hbm.10062>
- Smith, S. M., Fox, P. T., Miller, K. L., Glahn, D. C., Fox, P. M., Mackay, C. E., ... Beckmann, C. F. (2009). Correspondence of the brain's functional architecture during activation and rest. *Proceedings of the National Academy of Sciences of the United States of America*, 106(31), 13040–13045. <https://doi.org/10.1073/pnas.0905267106>
- Smith, S. M., Jenkinson, M., Woolrich, M. W., Beckmann, C. F., Behrens, T. E. J., Johansen-Berg, H., ... Matthews, P. M. (2004). Advances in functional and structural MR image analysis and implementation as FSL. *NeuroImage*, 23(Suppl 1), S208–S219. <https://doi.org/10.1016/j.neuroimage.2004.07.051>

- Spitzer, R. L., Williams, J. B., Gibbon, M., & First, M. B. (1992). The structured clinical interview for DSM-III-R (SCID). I: History, rationale, and description. *Archives of General Psychiatry*, 49(8), 624–629.
- Sporns, O. (2014). Contributions and challenges for network models in cognitive neuroscience. *Nature Neuroscience*, 17(5), 652–660. <https://doi.org/10.1038/nn.3690>
- Tagliazucchi, E., & Laufs, H. (2014). Decoding wakefulness levels from typical fMRI resting-state data reveals reliable drifts between wakefulness and sleep. *Neuron*, 82, 695–708. <https://doi.org/10.1016/j.neuron.2014.03.020>
- van den Heuvel, M. P., & Hulshoff Pol, H. E. (2010). Exploring the brain network: A review on resting-state fMRI functional connectivity. *European Neuropsychopharmacology: The Journal of the European College of Neuropsychopharmacology*, 20(8), 519–534. <https://doi.org/10.1016/j.euroneuro.2010.03.008>
- van der Werf, Y. D., Sanz-Arigita, E. J., Menning, S., & van den Heuvel, O. A. (2010). Modulating spontaneous brain activity using repetitive transcranial magnetic stimulation. *BMC Neuroscience*, 11, 145. <https://doi.org/10.1186/1471-2202-11-145>
- Van Dijk, K. R. A., Hedden, T., Venkataraman, A., Evans, K. C., Lazar, S. W., & Buckner, R. L. (2010). Intrinsic functional connectivity as a tool for human connectomics: Theory, properties, and optimization. *Journal of Neurophysiology*, 103(1), 297–321. <https://doi.org/10.1152/jn.00783.2009>
- Verhage, F. (1964). *Intelligentie en leeftijd; onderzoek bij Nederlanders van twaalf tot zeventenzeventig jaar*. Assen: Van Gorcum.
- Walker, D. (2003). JMASM9: Converting Kendall's tau for correlational or meta-analytic analyses. *Journal of Modern Applied Statistical Methods*, 2(2), 525–530. <https://doi.org/10.22237/jmasm/1067646360>
- Warren, D. E., Power, J. D., Bruss, J., Denburg, N. L., Waldron, E. J., Sun, H., ... Tranel, D. (2014). Network measures predict neuropsychological outcome after brain injury. *Proceedings of the National Academy of Sciences of the United States of America*, 111(39), 14247–14252. <https://doi.org/10.1073/pnas.1322173111>
- Yarkoni, T. (2009). Big correlations in little studies: Inflated fMRI correlations reflect low statistical power—Commentary on Vul et al. (2009). *Perspectives on Psychological Science*, 4(3), 294–298. <https://doi.org/10.1111/j.1745-6924.2009.01127.x>
- Yeo, B. T. T., Krienen, F. M., Sepulcre, J., Sabuncu, M. R., Lashkari, D., Hollinshead, M., ... Buckner, R. L. (2011). The organization of the human cerebral cortex estimated by intrinsic functional connectivity. *Journal of Neurophysiology*, 106(3), 1125–1165. <https://doi.org/10.1152/jn.00338.2011>
- Zhang, Y., Brady, M., & Smith, S. (2001). Segmentation of brain MR images through a hidden Markov random field model and the expectation-maximization algorithm. *IEEE Transactions on Medical Imaging*, 20(1), 45–57. <https://doi.org/10.1109/42.906424>

SUPPORTING INFORMATION

Additional supporting information may be found online in the Supporting Information section at the end of this article.

How to cite this article: Fitzsimmons SMDD, Douw L, van den Heuvel OA, van der Werf YD, Vriend C. Resting-state and task-based centrality of dorsolateral prefrontal cortex predict resilience to 1 Hz repetitive transcranial magnetic stimulation. *Hum Brain Mapp*. 2020;41:3161–3171. <https://doi.org/10.1002/hbm.25005>

APPENDIX A:

Image preprocessing steps

All image processing was performed using FMRIB's software library (FSL) version 5.0.8:

- Removal of nonbrain tissue using the Brain Extraction Tool (Smith, 2002).
- Grey and white matter segmentation using FAST (Zhang, Brady, & Smith, 2001).
- Parcellation into 225 regions in order to define nodes for graph analysis. We used the Brainnetome Atlas (Fan et al., 2016) to define 210 cortical regions; 14 subcortical areas were individually segmented using FSL FIRST (Patenaude, Smith, Kennedy, & Jenkinson, 2011); and one cerebellar ROI from FSL's cerebellar atlas was segmented (Diedrichsen, Balsters, Flavell, Cussans, & Ramnani, 2009).
- Preprocessing of fMRI data using the FSL MELODIC pipeline (Beckmann, DeLuca, Devlin, & Smith, 2005): discarding the first four volumes, motion correction, spatial smoothing (5 mm full width at half maximum), and high-pass filtering (100 s cut-off).
- Coregistration to T1-weighted anatomical MR scans using linear and nonlinear coregistration methods (Jenkinson, Bannister, Brady, & Smith, 2002).
- To account for EPI distortions near air/tissue boundaries during scanning, we applied a mask to the functional scan to exclude voxels with signal intensities in the lowest quartile of the robust range (Meijer et al., 2017). Any nodes containing <4 voxels were excluded. A total of 193 regions common to all fMRI runs remained: excluded regions were located in the orbitofrontal gyrus, inferior temporal gyrus, parahippocampal gyrus, and thalamus.
- Extraction of timeseries from each parcellated region.

APPENDIX B:

Subdivision into dIPFC-containing modules

Networks can be subdivided into groups of regions that are densely interconnected, known as modules or subnetworks. In the context of functional networks, they are thought to represent areas of segregated processing (Rubinov & Sporns, 2010), and specific modules may correspond to specific cognitive functions (Niendam et al., 2012). The Louvain modularity algorithm from the Brain Connectivity Toolbox (Rubinov & Sporns, 2010) (<https://sites.google.com/site/bctnet/>) was used to define dIPFC-containing modules for each participant individually, and for RS and each task-based run separately, as modularity is known to vary between individuals and between task and resting states (De Salvo, Douw, Takaya, Liu, & Stufflebeam, 2014). Since Louvain modularity is an heuristic algorithm, and produces slightly different subdivisions of nodes each time it is run (Lancichinetti & Fortunato, 2012), we permuted the algorithm 1,000 times, calculated pairwise similarities between all iterations, and used the iteration with the most similarity to all other iterations as a consensus network (Doron, Bassett, & Gazzaniga, 2012). A resolution parameter (γ) of 1.1 was used as this gave on average seven modules per participant, which is a previously described stable subdivision of known resting state functional networks (Yeo et al., 2011).